Wide Bandwidth Endfire Antenna with Log-Period Directors

Yuanhua Sun [1], Guangjun Wen [1], Haiyan Jin [1], Ping Wang [1,2], Yongjun Huang [1], and Jian Li [1]

[1] Centre for RFIC and System Technology, School of Communication and Information Engineering
University of Electronic Science and Technology of China, Chengdu 611731, China
sunyuanhua17@gmail.com

[2] Department of Electronic Engineering, College of Electronic and Information Engineering
Chongqing Three Gorges University, Chongqing 404000, China
cqrainycity@yahoo.com.cn

Abstract ─ This paper presents the design and implementation of a novel wide bandwidth endfire antenna with log-periodic directors. The feeding structure of the proposed antenna includes a balun which is formed using a pair of microstrip-to-slotline transitions. The proposed antenna has three resonant frequencies in the operating frequency band. Both simulation and measurement results show that the operating frequency band of the antenna for $S_{11} < -10$ dB covers the wide bandwidth (5 GHz – 10 GHz), and the relative bandwidth is 67%. Far field measurements in azimuth plane and elevation plane show that the radiation patterns are stable and end fire within the operating band at frequencies of 5 GHz, 7 GHz, 8 GHz, 10 GHz. The proposed antenna radiates a well-defined endfire beam, with a front-to-back ratio > 18 dB and cross polarization level below -28 dB. The dimension of the proposed antenna is 26 mm × 27 mm. Good return loss and radiation pattern characteristics are obtained and measured results are presented to validate the usefulness of the proposed antenna structure for wide bandwidth endfire applications.

Index Terms ─ Endfire antenna, front-to-back ratio, log-period directors, wide bandwidth antenna.

I. INTRODUCTION

The advantages of a printed endfire antenna include not only the characteristics of a radiational Yagi antenna with endfire radiation pattern [1], [2], but also the characteristic of a microstrip antenna with low profile, miniature size, easy fabrication and low cost [3-6]. The feeding structure of quasi-Yagi antenna plays the crucial role in the performance. The odd-mode excitation needed for the driver, which is in the form of a centre-fed dipole, has to be maintained over the whole bandwidth by using a suitable balun. Baluns that are based on different types of transitions [7-9]. In [10] and [11], a hook-shaped balun is proposed for the feed of the antenna. A broadband dipole antenna fed by an end-open "J" balun with integrated via-hole is presented in [12]. Due to the need to cover wide bandwidth, designs of endfire antennas focus on implementing new techniques aimed at increasing the bandwidth. The key factors to achieve wide bandwidth include using wide bandwidth baluns in the feeding structure of the antenna and modifying the shape of the radiator [13-15]. The maximum achieved bandwidth in those techniques is around 60% but the dimensions are large.

In this paper, the proposed antenna consists of the balun, driver, log-periodic directors and reflector in the form of truncated ground plane. The proposed antenna is compacted, the dimension of the proposed antenna is 26 mm × 27 mm. An ultra-wideband microstrip-to-coplanar stripline balun is presented. The proposed antenna is fed by the ultra-wideband balun. The proposed antenna includes tapered drivers, log-periodic directors and a truncated ground plane acting as a reflector. The antenna should find wide application in a great variety of wireless systems such as microwave imaging system.

As shown in Fig. 1, the configuration of the balun is a part of the complete antenna structure. The input port is converted from a microstrip line to a slotline using a wideband microstrip-to-slotline transition. The circular slots at the bottom layer and circular microstrip patch at the top layer are used to achieve the required impedance matching between the input microstrip line and the output slotline across an ultra-wideband. The slotline at the bottom layer is coupled to a coplanar stripline (CPS) at the top layer using another slotline to microstrip transition. The balun creates equal in magnitude and out-of-phase signals across a wide frequency band in the CPS output. The input microstrip line of the balun is designed to have 50 Ω impedance for a perfect matching with the input feeder. To simulate the characteristics of the designed antenna, we used the simulation software high frequencies in the operating

frequency bandwidth. The effects on each resonant frequency caused by the key antenna parameters such as the length of driven element, the length of director, the distance between the driven element and the director, the length of ground gap and diameter of the metal circle patch. Through optimizing three resonant frequencies, a wideband endfire antenna is designed and fabricated. Then, a series of measurements are conducted with a Vector Network Analyzer in an anechoic chamber. The measured results show that the relative bandwidth for S_{11} < -10 dB is about 67%. The radiation patterns at 5 GHz, 7 GHz, 8 GHz and 10 GHz also show that the antenna works well in an end-fire state and has a stable characteristic.

The taper driver and log-periodic directors are used to increase the operational bandwidth. In the presented design, a pair of microstrip-to-slotline transitions is used to feed the antenna and the size of the antenna is not increasing significantly. The performance of the designed antenna is simulated using the simulation tool HFSS v13. The antenna radiates a well-defined end-fire beam, with a front-to-back ratio (> 20 dB) and cross-polarization level below -18 dB.

II. ANTENNA DESIGN AND PARAMETERS STUDY

The configuration of the proposed end-fire antenna is shown in Fig. 1. The antenna is printed on Rogers RT6010LM substrate which has a thickness of 0.635 mm. The relative permittivity of the substrate is 10.2 and the dielectric loss tangent is 0.0023. The feeding structure consists of a 50 Ω microstrip connected to 50 Ω SMA connector, and a balun which is composed of two microstrip-to-slotline transitions and T-junction of microstrip slotline. The utilized transitions to form the balun are designed following the guidelines in [16].

The gap between the two arms of the driver is chosen for the best possible matching with coplanar stripline feeder of the driver. The driver of the proposed antenna is in the form of center-fed dipole with tapered width in the form of a bow-tie. The reflector is in the form of truncated ground. The feeding structure of the antenna includes a balun that is formed from two microstrip-to-slotline transitions and T-junction of microstrip/slotline. The driver is made up by taper arms with total length equal to half of the effective wavelength at the center of band. Directors in form of log-periodic rectangular arms are placed in front of the driver and at a distance between the ground plane and the driver. The overall dimensions of the proposed antenna and the feeding structure are optimized using the simulation tool HFFS v13. The overall dimensions of the antenna are 26 mm × 27 mm indicating a compact size.

(a)

(b)
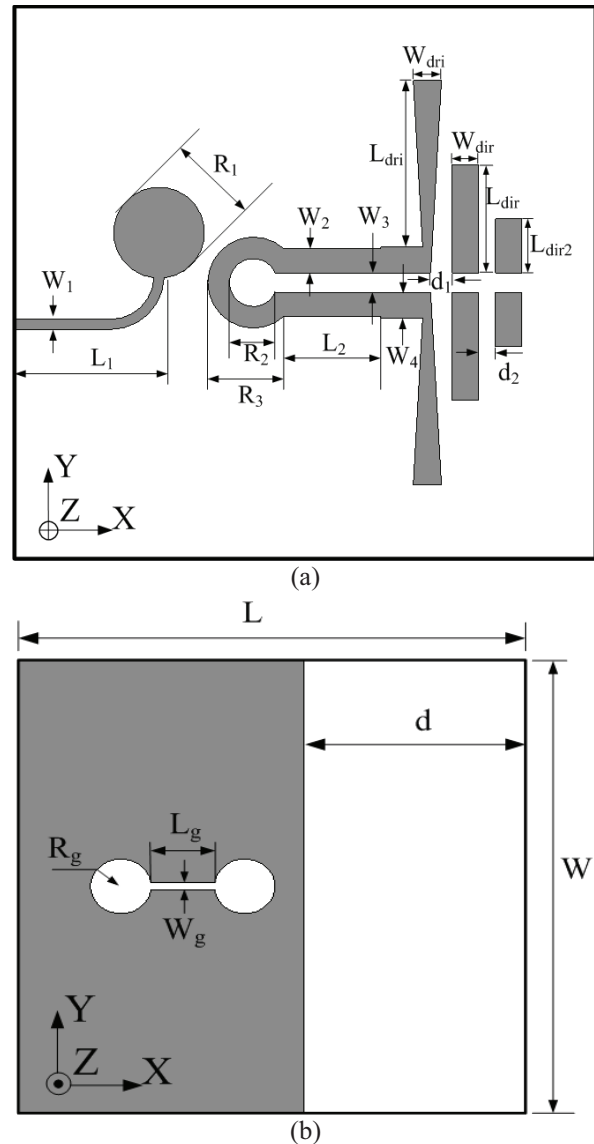
Fig. 1. Configuration of the proposed antenna: (a) front view, and (b) back view.

A. Effects of the driven element

L_{dri} becomes shorter than a quarter of wavelength at the first resonant frequency [17]. Figure 2 (b) shows the width of gap between two driver elements. From Fig. 2 (b), it is found that W_3 does significantly improve the bandwidth of the proposed antenna. The bandwidth defined by S_{11} < -10 dB increases when W_3 is decreased from 1.5 mm to 0.6 mm. However, when W_3 < 0.6 mm, the bandwidth changed badly. The simulation results show that all of the resonances from high frequencies to low frequencies shifted slightly while W_3 decreased. These results illustrate that the lowest operating frequency of the antenna depends primarily on the length L_{dri} and W_3.

(a)

(b)
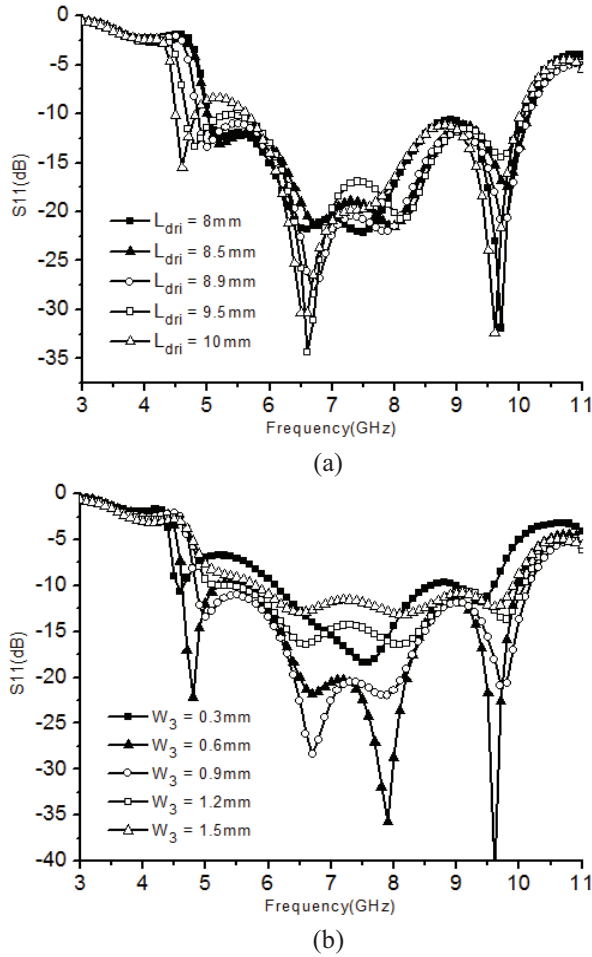
Fig. 2. Effects of the driven element: (a) simulated S_{11} with different L_{dri}, other parameters are the same as Fig. 1. (b) Simulated S_{11} with different W_3, other parameters is the same as Fig. 1.

B. Effects of the directors

The director of the traditional Yagi antenna obtains its energy by electromagnetic coupling from the driven element. The length of the director and the spacing relative to the driven element affect the gain and bandwidth of the Yagi antenna. According to [18], the typical length of the director is shortened by 10-20% from the length of the driver. The log-periodic directors are used to improve the bandwidth of the proposed antenna. The effects of the director are shown in Fig. 3.

Figure 3 (a) shows the S_{11} of the proposed antenna corresponding to different lengths of the first director element, L_{dir1}. From the Figure 3 (a), it can be observed that the third resonant frequency is significantly decreased such that the bandwidth of the proposed antenna becomes narrow when L_{dir1} is increased from 5 mm to 8 mm. From the Fig. 3 (b), it can be observed that the third resonant frequency decreased and the forth resonant frequency changed badly when W_{dir} is increased

from 0.5 mm to 2 mm. Therefore, the highest operating frequency of the antenna depends primarily on the length of the first director.

(a)

(b)
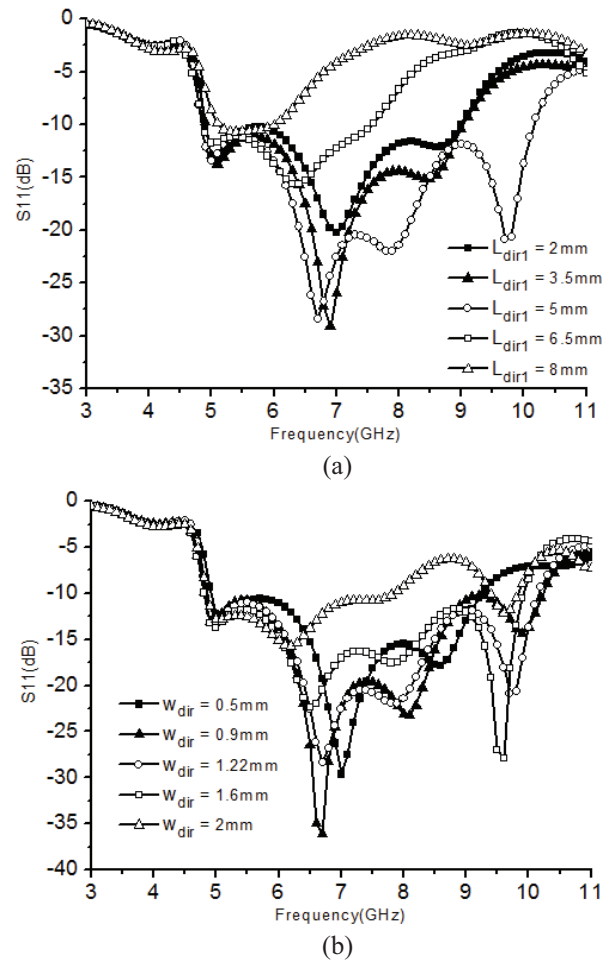
Fig. 3. Effects of the director: (a) simulated S_{11} with different L_{dir1}, other parameters are the same as Fig. 1. (b) Simulated S_{11} with different W_{dir}, other parameters is the same as Fig. 1.

C. Effects of the feeding system

Figure 4 shows the effects of the feed system of the antenna. The S_{11} of the proposed antenna corresponds to different lengths of the slotline transition, L_g in the ground plane, shown in Fig. 4 (a). Increasing L_g from 2.5 mm to 4 mm causes a decrease of the second resonant frequency. As a result, the impedance match becomes better within the low-frequency band, but it becomes worse within high-frequency band. Figure. 4 (b) shows the S_{11} with respect to the different diameters of the circle patch in the top layer, R_1.

Similar to the trend of L_g, increasing R_1 results in a decrease of the second resonant frequency and a better impedance match in the low-frequency band and a worse impedance match in the high-frequency band.

Figure 4 (c) shows the S_{11} with respect to the different diameters of the tap circle in the ground plane, R_s.

(a)

(b)

(c)
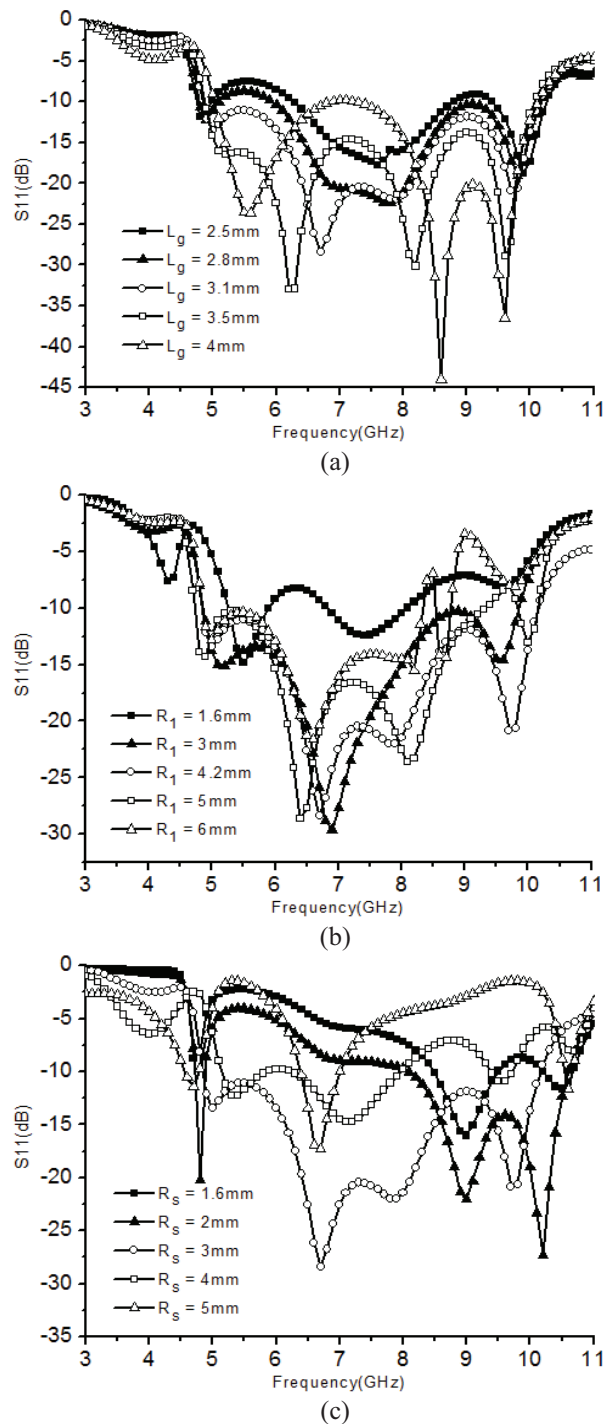
Fig. 4. Effects of the feed system: (a) Simulated S_{11} with different L_g, other parameters are the same as Fig. 1. (b) Simulated S_{11} with different R_1, other parameters are the same as Fig. 1. (c) Simulated S_{11} with different Rs, other parameters are the same as Fig. 1.

From the Fig. 4 (c), it can be observed that the third resonance is increased badly and the bandwidth of the proposed antenna becomes narrow when R_s is increased from 1.6 mm to 5 mm. Essentially, the second resonance and third resonance around the center of the operating frequency are determined by the feed structure.

III. SIMULATION AND MEASUREMENT RESULTS

According to the results discussed in the previous section, the optimal parameters of the proposed antenna are listed as follows: L=27 mm, W=26 mm, L_g=3.1 mm, L_{dri}=8.9 mm, L_{dir1}=6.5 mm, L_{dir2}=2.5 mm, W_{dri}=1.3 mm, W_{dir}=1.22 mm, W_3=0.9 mm, R_1=4.2 mm, R_s=3 mm, R_2=2.1 mm R_3=3.5 mm, W_1=0.46 mm, W_2=1.1 mm, W_3=0.9 mm, W_4=1.2 mm, L_1=7 mm, L_2=4.48 mm, d_1=1.0 mm, d_2=0.78 mm. To verify the proposed antenna design, a prototype is fabricated as shown in Fig. 5 and the results are presented here.
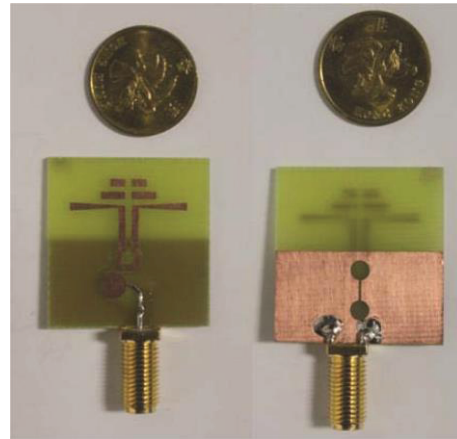
Fig. 5. Fabricated prototype of the proposed antenna.

All the measured results are carried out in anechoic chamber using a vector network analyzer (VNA) and other microwave test instruments. The variations of the reflection coefficient and gain with frequency are shown in Fig. 6. As shown in Fig. 6, the S_{11} from the measurement is compared with the simulation results, which shows accordance between measured and simulated values. The operating frequency defined by S_{11} < -10 dB ranges from 5 GHz to 10 GHz, and the relative bandwidth of the proposed antenna is 67%.

Within the operating frequencies, the measurement gain of the antenna is between 3 dB and 7.5 dB, as shown in Fig. 6. It is possible to increase the gain, if required, by adding director, but this would be at the cost of increasing the size of the antenna slightly. Co- and cross-polarization of far field radiation patterns in the E- and H-plane at 5 GHz, 6 GHz, 7 GHz, and 8 GHz were measured and plotted in Fig. 7. As shown in Fig. 7,

a well-defined end-fire pattern is observed with a front-to-back ratio of 18 dB and a maximum cross-polarization level of -28 dB. It is clear that the antenna has a reasonable directivity where the front-to-back ratio varies from around 7 dB to 10 dB across the 67% bandwidth. It can be observed from the figure that the radiation patterns are stable at these four operating frequencies in the xoy and xoz planes. The antenna works in an endfire state and the maximum radiation in the direction of the +x axis.
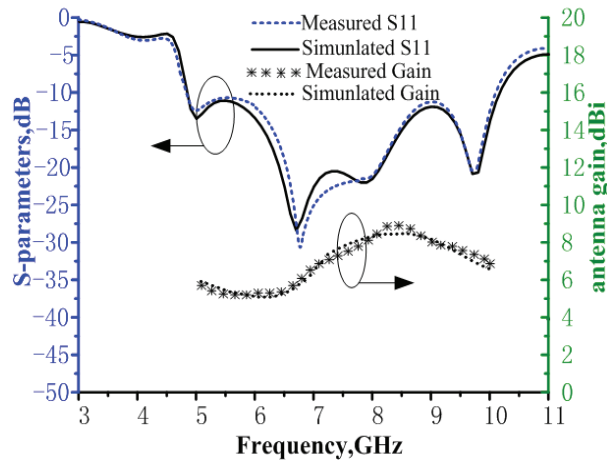
Fig. 6. The simulation and measurement reflection coefficient and measured gain.

(a)

(b)

(c)

(d)
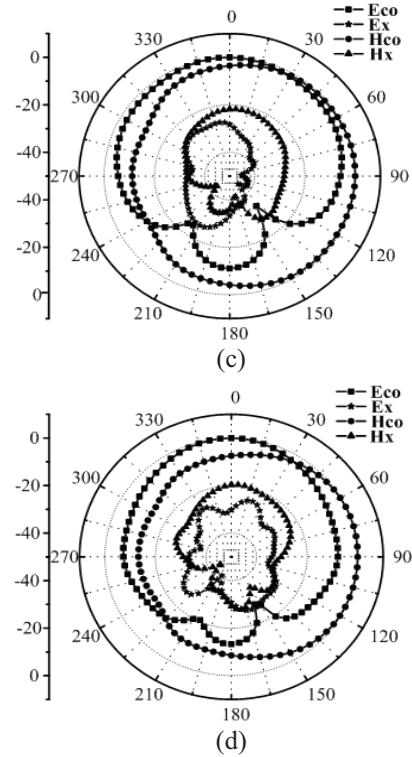
Fig. 7. The measured radiation pattern: (a) 5 GHz, (b) 7 GHz, (c) 8 GHz, and (d) 10 GHz.
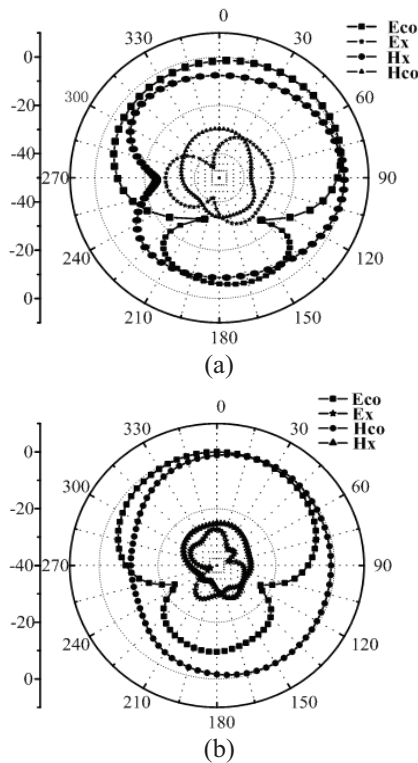
IV. CONCLUSION

In this paper, a novel endfire wide bandwidth antenna with log-periodic directors has been presented. The antenna is compact and easy to fabricate, and achieves extremely wide bandwidth and good radiation characteristics in items of beam pattern, front-to-back ratio and cross-polarization. Both simulation and measurement results show that the antenna achieves a relative frequency bandwidth of 67%. The stable radiation patters at 5, 7, 8, 10 GHz show that the antenna works in an endfire state and that the maximum radiation is in the direction of the +x axis. The front-to-back ratio of the proposed antenna is more than 28 dB. The cross polar performance is good and better than -18 dB. Further improvement to the radiation pattern and gain would require an additional director element. The antenna should find wide application in a great variety of wireless systems such as microwave imaging system.

REFERENCES

[1] P-Y. Qin, A. R. Weily, Y. J. Guo, T. S. Bird, and C-H. Liang, "Frequency reconfigurable quasi-Yagi folded dipole antenna," *IEEE Transactions on Antennas and Propagation*, vol. 58, pp. 2742-2747, 2010.

[2] N. Nikolic and A. R. Weily, "Compact E-band planar quasi-Yagi antenna with folded dipole driver," *IET Microwaves, Antennas & Propagation*, vol. 4, pp. 1728-1734, 2010.

[3] B. Honarbakhsh and A. Tavakoli, "Analysis of thin microstrip antennas by meshless methods," *The Applied Computational Electromagnetic Society*, vol. 27, pp. 983-990, 2012.

[4] Y. Li, P. Yang, F. Yang, and S. He, "A method to reduce the back radiation of the fold PIFA antenna with finite ground," *The Applied Computational Electromagnetic Society*, vol. 28, pp. 110-115, 2013.

[5] M. Ojaroudi, N. Ojaroudi, and N. Ghadimi, "Enhanced bandwidth small square slot antenna with circular polarization characteristrics for WLAN/WIMAX and C-band applications," *The Applied Computational Electromagnetic Society*, vol. 28, pp. 156-161, 2013.

[6] Y. Li, W. Li, and W. Yu, "A multi-band/UWB MIMO/diversity antenna with an enhanced isolation using radial stub loaded resonator," *The Applied Computational Electromagnetic Society*, vol. 28, pp. 8-20, 2013.

[7] Z. P. Wang, "Yagi antenna with improved out-of-band gain suppression," *IET Electronics Letters*, vol. 48, pp. 546-548, 2012.

[8] T-G. Ma, C-W. Wang, R-C. Hua, and J-W. Tsai, "A modified quasi-Yagi antenna with a new compact microstrip-to-coplanar strip transition using artificial transmission lines," *IEEE Trans. Antenna Propag.*, vol. 57, pp. 2469-2474, 2009.

[9] H. K. Kan, A. M. Abbosh, R. B. Waterhouse, and M. E. Bialkowski, "Compact broadband coplanar waveguide-fed curved quasi-Yagi antenna," *IET Microw. Antennas Propag.*, vol. 3, pp. 572-574, 2007.

[10] S. J. Wu, C. H. Kang, K. H. Chen, and J. H. Tarng, "A multiband quasi-Yagi type antenna," *IEEE Transactions on Antennas and Propagation*, vol. 58, pp. 593-596, 2010.

[11] D. C. Chang, C. B. Chang, and J. C. Liu, "Modified planar quasi-Yagi antenna for WLAN dual-band operation," *Microwave and Optical Technology Letters*, vol. 46, pp. 443-446, 2005.

[12] E. A. Navarro, B. Schoenlinner, and G. M. Rebeiz, "Broadband printed dipole with integrated via-hole balun for WiMAX applications," *Microwave and Optical Technology Letters*, vol. 53, pp. 52-55, 2011.

[13] Z. Y. Zhang, G. Fu, S. L. Zuo, and X. Gong, "Wideband unidirectional patch antenna with Γ–shaped strip feed," *Electronics Letters*, vol. 46, pp. 24-26, 2010.

[14] N. K. Nahar, B. Raines, R. G. Rojas, and B. Strojny, "Wideband antenna array beam steering with free-space optical true-time delay engine," *IET Microwaves, Antennas & Propagation*, vol. 5, pp. 740-746, 2011.

[15] H. Kan, R. Waterhouse, A. Abbosh, and M. Bialkowski, "Simple broadband planar CPW-fed quasi-Yagi antenna," *IEEE Antennas Wireless Propag. Letters*, vol. 6, pp. 18-20, 2007.

[16] M. E. Bialkowski and A. M. Abbosh, "Design of a compact UWB out-of-phase power divider," *Progress In Electromagnetics Research*, vol. 116, pp. 18-20, 2007.

[17] O. Tze-Meng, K. G. Tan, and A. W. Reza, "A dual-band omni-directional microstrip antenna," *Progress In Electromagnetics Research*, vol. 106, pp. 363-376, 2010.

[18] W. L. Stutzman and G. A. Thiele, *Antenna Theory and Design*, New York, Wiley, 1998.

Yuanhua Sun received the B.S. degree in Communication Engineering from the Liaocheng University in 2007, and M.S. degree in Signal and Information Processing from Chengdu University of Information Technology in 2010. He is working toward the Ph.D. degree in UESTC. His research interests include analytical and numerical modeling of metamaterials and antenna theory and design and signal processing.

Guangjun Wen was born in Sichuan, China, in 1964. He received his M.S. and Ph.D. degrees in Chongqing University of China in 1995 and UESTC in 1998, respectively. He is currently a Professor and Doctor Supervisor in UESTC.

His research and industrial experience covers a broad spectrum of electromagnetics, including RF, Microwave, Millimeter wave Integrated Circuits and Systems design for Wireless Communication, Navigation, Identification, Mobile TV applications, RFIC/MMIC/MMMIC device modeling, System on Chip (SoC) and System in Package (SiC) Design,

RF/Microwave/Millimeter wave Power source Desdgn, "The Internet of things" devices and system, RFID system and networks, antennas, as well as model of electromagnetic metamaterial and its application in microwave engineering area.

Haiyan Jin received the M.S. and Ph.D. degrees in Electrical Engineering and Communication and Information Engineering from University of Electronic Science and Technology of China in 2006 and 2010, respectively. He now is Associate Professor with School of Communication and Information Engineering, University of Electronic Science and Technology of China.

Ping Wang received the B.S. degree in Physics from Western Chongqing University of China in 2005 and the M.S. degree in Theoretical Physics from Chongqing University, Chongqing, in 2008. Currently, he is working toward the Ph.D. degree in UESTC. His current research interests include patch antennas, wideband antennas, and arrays.

Yongjun Huang received the B.S. degree in Mathematics from Neijiang Normal University of China in 2007, M.S. degree in Communication Engineering from University of Electronic Science and Technology of China (UESTC) in 2010, and is currently working toward a Ph.D. degree in UESTC. His research activities are electromagnetic metamaterial and its application in microwave engineering area, FDTD and CAD analysis for the metamaterial model and characteristics.

Jian Li received the B.S. and M.S. degrees in Communication Engineering from UESTC in 2007 and 2010, respectively, and is currently working toward a Ph.D. degree in UESTC. His research interests include RF, Microwave, and Millimeter wave Integrated Circuits and system. His is also interested in electromagnetic metamaterial and its applications in substrate integrated waveguide.